Calcif Tissue Int (1997) 60:361–367

Calcified Tissue International

Laboratory Investigations

X-ray Pole Figure Analysis of Apatite Crystals and Collagen Molecules in Bone

N. Sasaki,[1] Y. Sudoh[2]

[1]Division of Biological Sciences, Graduate School of Science, Hokkaido University, Kita-Ku Sapporo 060, Japan
[2]Department of Applied Chemistry, Muroran Institute of Technology, Mizumoto, Muroran 050, Japan

Received: 2 May 1996 / Accepted: 24 September 1996

Abstract. X-ray pole figure analysis was performed on apatite (AP) crystals in bone mineral and collagen molecules in the bone matrix. For AP in bone mineral, the (0002) plane (c-axis) and {21$\bar{3}$0} plane were examined. The diffraction peaks from both planes were well isolated from other diffraction peaks in the bone. To investigate the orientation of collagen molecules in the bone matrix, demineralized bone by EDTA treatment was used. For collagen, the diffraction peak from about the 0.3 nm period along the helix axis of the collagen molecule was investigated. The c-axis of AP and the helical axis of the collagen molecule have strongly preferred orientations in a direction parallel to the bone axis. The c-axis of AP has an appreciable pole density peak in the radial and tangential direction of the bone, whereas collagen molecules were almost uniaxially oriented in the bone axis direction though having an appreciable distribution. This suggests that there are more than two types of morphology in the AP particle in bone mineral: one with the c-axis almost parallel to the bone axis and the other in which the c-axis is oriented almost perpendicular to the bone axis. The {21$\bar{3}$0} plane has isolated peaks of pole density in pole figures in both radial and tangential directions. On the basis of the classification of orientation for elongated polyethylene, the main portion of AP particles in bone is concluded to be biaxially oriented.

Key words: Mineral orientation — Mineral morphology — Collagen fiber orientation — X-ray pole figure analysis.

Bone has long been regarded as a composite material of collagen and apatite (AP) mineral particles [1, 2]. Young's modulus of AP is about 80 times that of collagen [3, 4]. It is thought that the pliant collagen matrix is reinforced by stiff mineral particles and as a composite, the brittleness of the mineral is compensated by the pliancy of the matrix. The AP crystal has a hexagonal symmetry, although earlier studies [5, 6] and recent X-ray diffraction studies [7] considered the shape of AP particles in bone to be needle-like or rod-like; later electron micrograph investigations of the bone revealed that mineral particles are tabular shaped [8–10] or elongated platelets [11]. These revelations of the microscopic structure in bone indicate the importance of mineral orientation in the mechanical properties of bone [12–14]. The c-axis of the AP crystal has been revealed to be generally parallel to the longest dimension of the mineral particle [12]. A comparison of the results of X-ray pole figure analysis (XPFA) [12] and small angle X-ray scattering (SAXS) [15], however, has shown that some mineral particles have their c-axes perpendicular to their longest dimension, as predicted by Lees [16]. On the other hand, it has been reported that the collagen molecule plays an important role in mineral precipitation in bone as a promoter of the calcification reaction [11, 17]. The relationship between mineral and collagen is expected to be reflected in the geometrical arrangement of the two components.

The aim of this study was (1) to investigate the relationship between the preferred orientations of mineral particles and collagen molecules in bone by XPFA. The polar distribution of the c-axis of AP of bone and the helix axis of collagen molecule in bone were measured; and (2) to investigate the crystallographic axis, which is perpendicular to the c-axis of AP, in order to clarify whether the orientation of AP mineral particles are uniaxial or biaxial. To investigate the collagen molecular orientation in the bone matrix, XPFA for fully demineralized bone collagen was performed. This demineralization is necessary because the diffraction peak corresponding to the 0.3 nm period from the collagen lattice in the bone matrix is hidden by the diffraction peaks from AP planes such as {21$\bar{3}$1}, {11$\bar{2}$2}, {30$\bar{3}$0}. The fibril structure of collagen in bone and the general orientation of collagen molecules still remained after demineralization by EDTA [18].

X-ray Pole Figure Analysis

Pole figures are stereographic projections showing the density of crystallographic poles of certain planes as a function of orientation, and so provide a good method of representing orientation. A pole is the point of intersection of the normal to a crystal plane with the surface of a sphere having the crystal at its center. If the radius of the sphere is r = 1/d(hkl), the pole coincides with the reciprocal lattice point of this plane, and the density of the poles on the surface of the sphere is a faithful representation of the reciprocal lattice point density distribution. As an actual stereographic projection diagram, a polar net is generally used.

The scattering intensity is measured as a function of two

Correspondence to: N. Sasaki

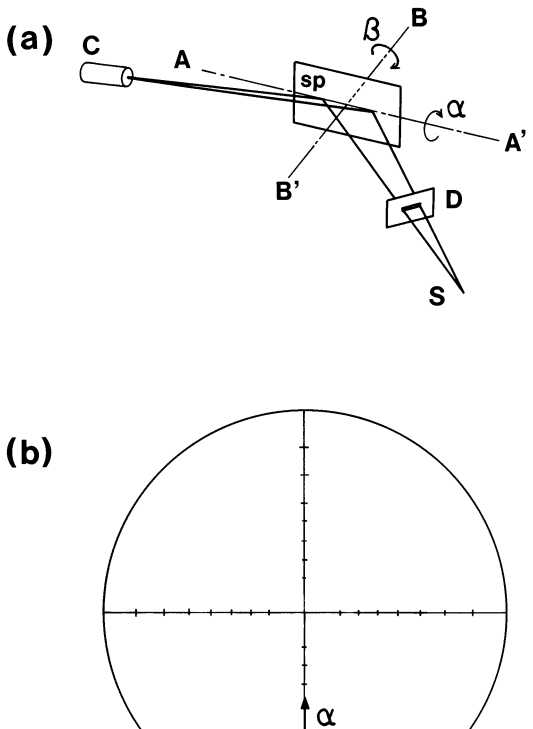

Fig. 1. (a) Schematic drawing of XPFA apparatus. X-ray detector, (C) specimen (sp), Schultz slit (D), and X-ray source (S), are aligned and fixed at the Bragg angle 2 θ_{hkl} for the plane (hkl) of interest. sp is rotated around AA′ and BB′ axes. The rotation angles are defined as α and β, respectively, where $0° < \alpha < 90°$ and $0° < \beta < 360°$. **(b)** Diffracted intensity from (hkl) plane is plotted in the polar net as a function of angular coordinates α and β. When the plane made by S, D, and C is perpendicular to sp plane, α is defined as 90° and the intensity I(α,β) is plotted at the center of the polar net.

angular coordinates, α and β, which are rotation angles of the specimen plane around the axes A and B, respectively, and which correspond to radial (declinational) and circumferential (azimuthal) coordinates, respectively, in a polar net (Fig. 1a, b). At the center of the polar net, $\alpha = 90°$, and at the outermost circle, $\alpha = 0°$.

If the crystallite orientation is completely random, the poles will be scattered all over the polar net. If the orientation is present, on the other hand, the poles will tend to be concentrated in certain areas within the polar net and the remaining areas will be completely unpopulated. The degree of orientation can also be found from the pole density.

Materials and Methods

Bone specimens were prepared from the femur of a 20 month-old cow, which was obtained immediately after slaughter. An optical microscopic examination showed that all of the samples were generally plexiform bone but partly remodeled into the Haversian system. The surfaces of the specimens for X-ray measurements were cut by a band saw, then filed by emery paper and finally polished by apatite paste. Both cutting and filing were performed under running tap water. The collagen matrix specimens were prepared by treating the same bovine femur with EDTA; the demineralizing reaction was performed with 0.5 M EDTA at pH 8.0 and 4°C for 2 weeks, and the EDTA solution was exchanged every day [18].

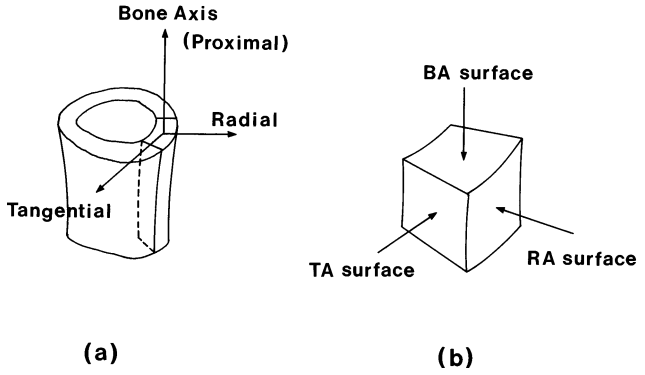

Fig. 2. (a) Cartesian coordinate system chosen for cortical bone specimens. **(b)** Three surfaces based on the Cartesian coordinate defined in **(a).** XPFA were made for these surfaces.

Complete demineralization was verified by X-ray diffraction which showed that the characteristic apatite diffraction pattern had disappeared from the specimen.

As shown in Figure 2a, a right-handed rectangular coordinate system was assumed to exist in the bone. XPFA was performed for three surfaces perpendicular to these three axes (Fig. 2b), referred to as BA surface, RA surface, and TA surface which are perpendicular to bone axis, radial axis, and tangential axis, respectively. These axes were specified by eye measurement.

Apparatus

X-ray pole figure analysis was performed using a Rigaku Denki Pole Figure Analyzing System with a Rad C computing system. A 30 kV 40 mA Cu K α X-ray beam was generated by a Rigaku Denki RU200 generator. The X-ray beam was monochromatized by a curved Si crystal monochrometer.

In order to investigate the relationship of preferred orientation between mineral particles and collagen, the (0002) pole distribution was investigated as a measure of the c-axis orientation of the AP mineral particle. To investigate the fiber orientation in the collagen matrix, the 0.3 nm period in the fiber axis direction relating to helix pitch of collagen was used as a probe [20]. Planes with a θ Bragg angle well isolated from other peaks give optimum results. Both the (0002) plane for AP and the 0.3 nm period for collagen give well-isolated reflections.

In order to examine the orientation of the crystallographic axis of AP perpendicular to the c-axis, {$2\bar{1}30$} reflection was used because of the suitable intensity. {$10\bar{1}2$} reflection locates near {$2\bar{1}30$}. In the intensity at the peak of {$2\bar{1}30$} reflection there may be a slight contribution of foot of the {$10\bar{1}2$} reflection. Such a contribution, however, does not affect significantly the result if bone mineral particles are uniaxial or biaxial.

Schultz's reflection technique was used for the bone specimens, and collagen measurements were carried out by Schultz's transmission method [21]. Measurements were performed over the angle ranges $0° < \alpha < 90°$ and $0° < \beta < 360°$ with a correction using bone powder for estimating intensity from randomly orienting HAP. The intensity of the bone sample was normalized by the obtained intensity of random orientation. A spiral pitch of 5° (5° increase in α per 360° rotation of β) was combined with a suitable scanning speed. From the data thus obtained, $0° < \alpha < 60°$ for the reflection method and $30° < \alpha < 90°$ for the transmission method were used in the analysis to avoid inaccuracies in the data out of these α regions.

X-ray pole figure measurements were carried out on 27 bone specimens and 9 bone collagen specimens. Typical pole figure results for each surface are presented in the following section.

Results and Discussion

Orientations of the c-axis of AP in Bone

In Figure 3a, b, and c, pole figures for the (0002) plane of

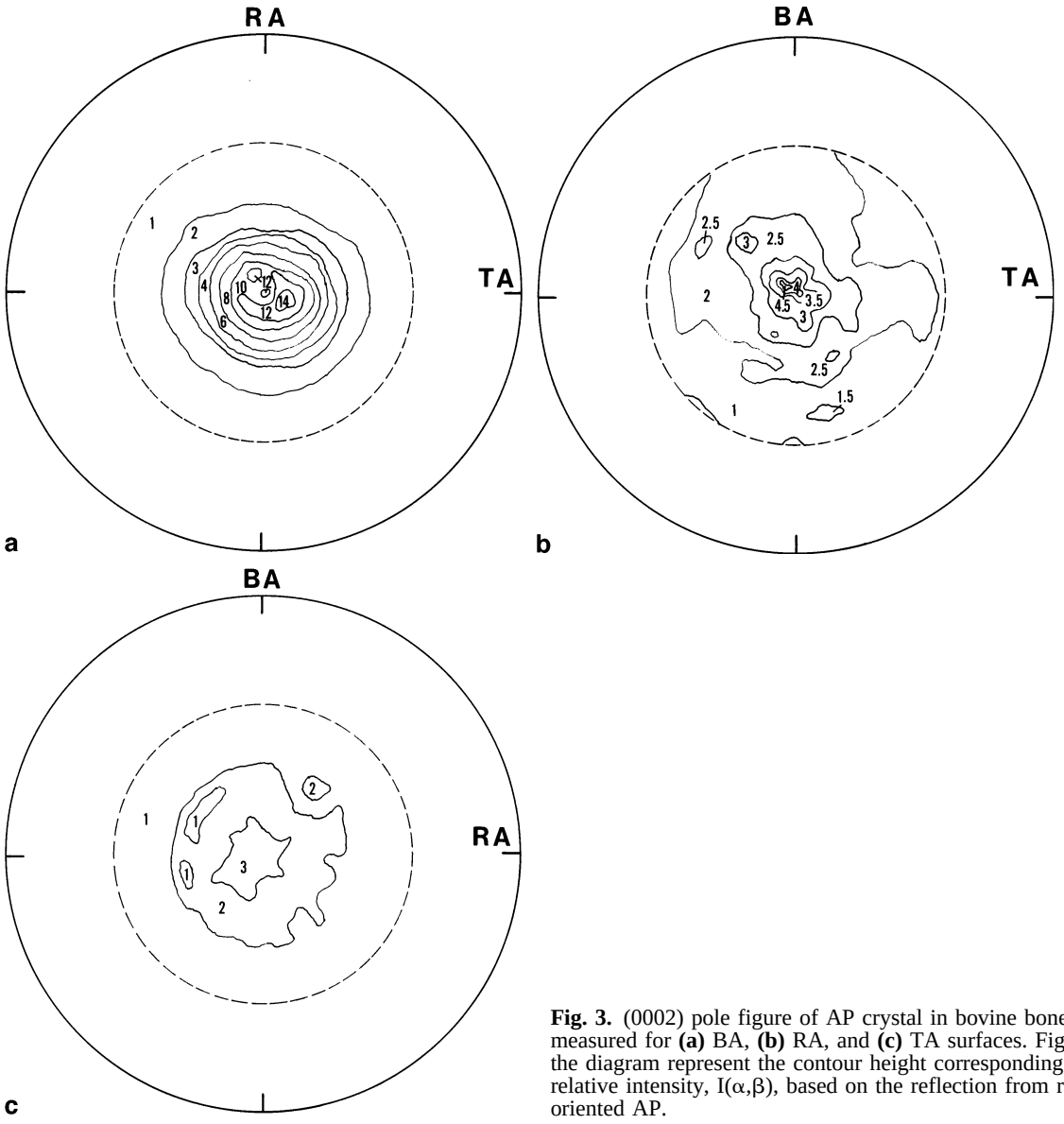

Fig. 3. (0002) pole figure of AP crystal in bovine bone mineral measured for **(a)** BA, **(b)** RA, and **(c)** TA surfaces. Figures in the diagram represent the contour height corresponding to the relative intensity, I(α,β), based on the reflection from randomly oriented AP.

AP in bone mineral are shown on the basis of the stereographic polar projection for the BA surface, RA surface, and TA surface, respectively. In each pole figure, the value of contour lines represents the normalized intensity I_n (α,β), of (0002) reflection of AP in bone mineral. The normalization was made by the intensity from a powdered bone specimen, I_p (α,β), as I_n (α,β) = I(α,β)/I_p (α,β), where I(α,β) is the intensity from the specimen. I_n (α,β) is proportional to the number of the normal vectors of (0002) planes orienting to the direction (α,β) in a real space. As the normal vector of a plane is defined as the pole of the plane, we call the number the pole density of (0002) plane. At the BA surface, the pole density of (0002) of AP in bone was larger in the center of the diagram. The contour lines were generally concentric and slightly elongated in the TA direction. In the pole figures for the RA and TA surfaces, the pole density of (0002) of AP in bone was larger in the center of the figure. The contour lines were found to be elliptical where the long axis of the ellipse was approximately parallel to the bone axis.

Figure 4a and b shows the sectional profiles of the pole figure for the BA surface (Fig. 3a), cut at the planes containing the BA and RA axes (β = 90°) and the BA and TA axes (β = 0°), respectively. In both figures, for 90° > α > 45°, the intensity of the pole figure of the BA surface was used. In Figure 4a, for 45° > α > 0°, the intensity of the pole figure of the RA surface was used, and for the same α region in Fig. 4b, the TA pole figure intensity was used. It was found that the intensity, I(α,β = 0° or 90°), in both cases decreased rapidly as the angle α decreased and I(α,β) took a minimum at about α = 45°, and gradually increased as α decreased to 0°.

These features of pole figures are in accordance with the results of our previous study [12], i. e., the c-axis of AP in bone which is normal to the (0002) plane is generally oriented parallel to the bone axis and a certain amount (~30% of all crystalline mineral particles) of c-axis of AP is also oriented in a direction perpendicular to the bone axis.

Orientation of the Fiber Axis of Collagen in Bone Matrix

As noted in the beginning of this paper, the fibril structure

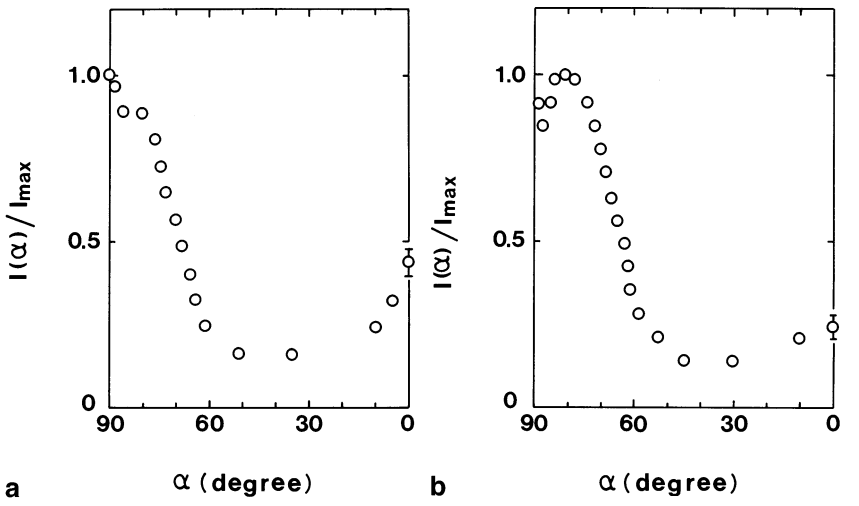

Fig. 4. The sectional profiles of the pole figure for the BA surface (Fig. 3a) cut at the planes containing the BA and RA (β = 90°) axes **(a)** and the BA and TA (β = 0°) axes **(b)** constructed by Figure 3 a and b and Figure 3 a and c, respectively.

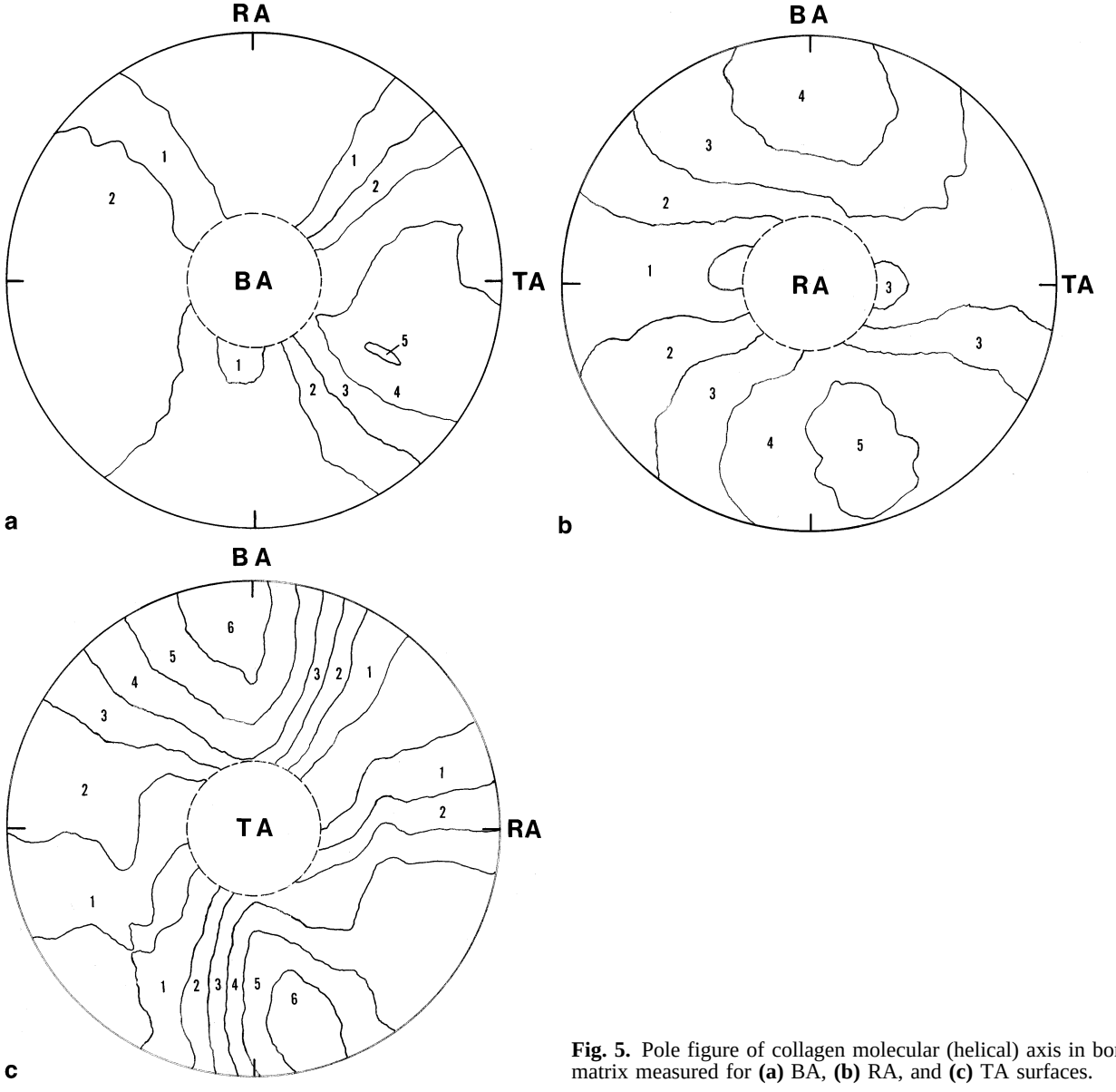

Fig. 5. Pole figure of collagen molecular (helical) axis in bone matrix measured for **(a)** BA, **(b)** RA, and **(c)** TA surfaces.

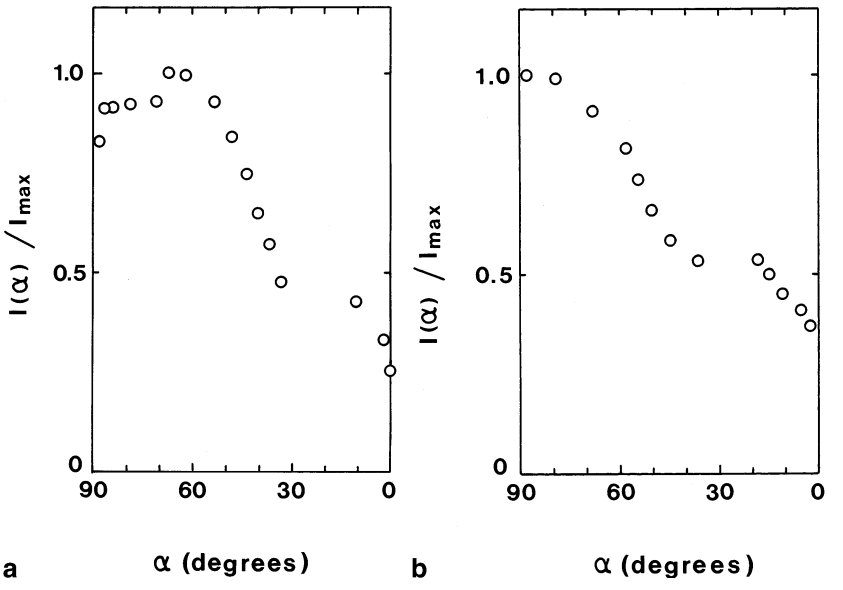

Fig. 6. The sectional profiles of the pole figure for the BA surface (Fig. 5a) cut at the planes containing the BA and RA ($\beta = 90°$) axes **(a)** and the BA and TA ($\beta = 0°$) axes **(b)** constructed by Figure 5 a and b and Figure 5 a and c, respectively.

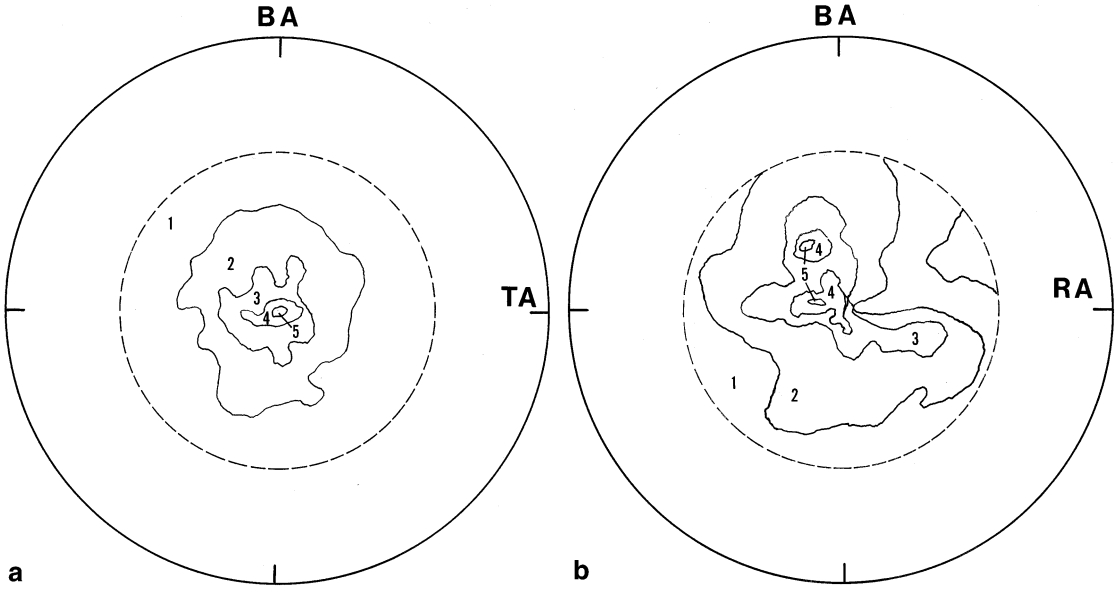

Fig. 7. {21$\bar{3}$0} pole figure of HAP crystal in bovine bone mineral measured for **(a)** RA and **(b)** TA surfaces.

of collagen in bone, and especially the general orientation of collagen molecules, remains after deminerlization by EDTA [18]. Figure 5a, b, and c, shows the pole figures for fiber axis of collagen in the bone matrix, based on the stereographic polar projection for the BA surface, RA surface, and TA surface, respectively. In each pole figure, the value of the contour lines also represents the normalized intensity $I(\alpha,\beta)$, of the fiber axis. It is clear that the fiber axis of collagen in the bone matrix also has a preferred orientation, although there is a pole density distribution. The preferred direction of the fiber axis of collagen is almost parallel to the bone axis with appreciable tilts to the TD and RD directions. The distribution of the pole density for the fiber axis of collagen is much broader than that for the c-axis of HAP in bone mineral. This result is in accord with the observation that collagen fiber orientation is more random in bone than in tendon [19]. The broadness of the distribution for the fiber axis of bone collagen is considered to be caused by local meandering, kink, and twisting of collagen fibers in the bone matrix. The difference in collagen matrix organization between bone and tendon is considered to be cellular in origin.

Figure 6 shows the sectional profiles of the pole figure for the BA surface (Fig. 5a), cut at the planes containing the BA ($\alpha = 90°$) and RA axes ($\alpha = 0°$, $\beta = 90°$) and the BA ($\alpha = 90°$) and TA axes ($\alpha = 0°$, $\beta = 0°$). Each curve was constructed by two pole figures obtained by transmission methods. In both Figures, for $45° > \alpha > 0°$, the intensity of the pole figure of the BA surface was used. In Figure 6a, for $90° > \alpha > 45°$, the intensity of the pole figure of the RA surface was used, and for the same α region in Figure 6b, the TA pole figure intensity was used. Intensity decreased almost continuously with a decrease in α from the BA direction ($\alpha = 90°$) to the RA or TA directions ($\alpha = 0°$).

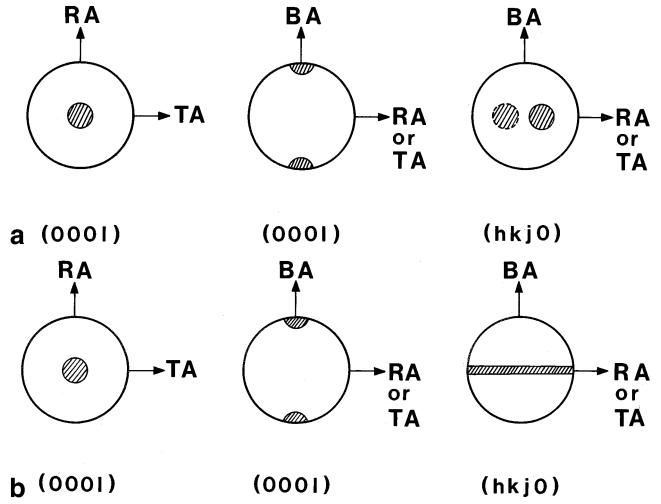

Fig. 8. Pole figures for two types of orientation: **(a)** biaxial orientation and **(b)** uniaxial orientation. In each figure, three schematic pole figures are shown: BA (left), TA or RA (center) surfaces for (0001) plane, and TA or RA surface for (hkj0) plane (right).

This result contrasts with those for HAP in bone mineral. In RA or TA directions, there were appreciable amounts of pole densities of AP (0002) plane. The profile of the pole figure for the collagen fiber axis is, however, similar to the orientational distribution function of the longest dimension of AP crystalline particles in bone determined by SAXS experiments [13]. The discrepancy and the coincidence between results for collagen fiber orientation and AP c-axis orientation suggest that there must be two types of morphology in AP crystalline particles; (1) most of the crystalline particles of AP have their c-axis parallel to the fiber axis of the collagen matrix [Type 1]; but (2) some of the AP particles in bone have their c-axis perpendicular to the collagen fiber axis [Type 2], though in both types of the particles, their length is parallel to the collagen fiber axis. From Figure 5a and b, the fractions of two types were estimated by assuming that the pole density profiles as a function of α, and is described by the linear combination of two gaussian-type distribution functions:

$$I_R(\alpha) = a_1 \exp(-b_1 \alpha^2) + a_2 \exp(-b_2 \alpha^2) \qquad (1)$$

where a and b are constants determined empirically, and subscripts represent the Type 1 and Type 2. The fractions of the type 1, ϕ_1 and the type 2, ϕ_2, are obtained as

$$\phi_j = a_j(\pi/b_j)^{1/2}/[a_1(\pi/b_1)^{1/2} + a_2(\pi/b_2)^{1/2}] \quad (j = 1 \text{ or } 2) \qquad (2)$$

The preliminary result was $\phi_1 = 0.7$ and $\phi_2 = 0.3$. In XPFA of bone, the number and the spacial distribution of crystalline mineral particles were measured. The crystallinity of bone minerals was estimated to be about 60% of the minerals [22], where 40% of the minerals are considered also to be crystallites but in the form of small particles or crystallites with remarkable imperfection. Thus, the fraction of type 2 AP crystal against all of the mineral in bone should be $0.6 \times 0.3 = 0.18$. According to Katz and Li [18], 70–80% of the mineral content must be within the fibrils, and Glimcher [23] presented evidence that up to 95% of the mineral may be intrafibril. The fraction of type 2 AP crystal to all the mineral in bone falls into the range for the fraction of mineral existing in interfibrillar space. This result confirms the model for the morphology of AP particles in bone proposed by Lees [16].

Table 1. Angles made by normal vectors (poles) of crystallographically equivalent planes belonging to $\{21\bar{3}0\}$

	$21\bar{3}0$	$12\bar{3}0$	$1\bar{3}20$	$2\bar{3}10$	$\bar{3}210$	$\bar{3}120$
$21\bar{3}0$	0°					
$12\bar{3}0$	21.78	0				
$1\bar{3}20$	120.00	141.78	0			
$2\bar{3}10$	98.22	120.00	21.78	0		
$\bar{3}210$	120.00	98.22	120.00	141.78	0	
$\bar{3}120$	141.78	120.00	98.22	120.00	21.78	0

Orientation of $\{21\bar{3}0\}$ Plane

Figure 7a and b shows the distribution of the $\{21\bar{3}0\}$ pole for RA and TA surfaces, respectively. In each surface, there is a pole density peak at about the center of the pole figure. The contour lines indicating the pole density are concentric and form ellipses in each pole figure where the longer axes of the ellipses lie between BA and RA or TA directions. In the case of elongated polyethylene, the orientation of the fiber axis was classified on the basis of the patterns of the two pole figures for {001} and {hk0} [24]. Figure 8 shows the classification of the orientation modified to bone mineral orientation. According to this classification, the type of orientation of AP crystals in bone is concluded to be biaxial orientation. $\{21\bar{3}0\}$ of AP has six crystallographically equivalent planes: $(21\bar{3}0)$, $(12\bar{3}0)$, $(2\bar{3}10)$, $(1\bar{3}20)$, $(\bar{3}210)$, and $(\bar{3}120)$. The angles made by two normals of $\{21\bar{3}0\}$ planes are estimated by a geometric calculation, and they are listed in Table 1. The pole of the plane belonging to the $\{21\bar{3}0\}$ group is thought to orient in the RA direction, and the pole of the other plane in the $\{21\bar{3}0\}$ group points in the direction near TA. The broadness of the pole density peak for $\{21\bar{3}0\}$ is attributed to the multiplicity of the $\{21\bar{3}0\}$ plane group as well as the distribution in the pole orientation. Thus, in pole figures for both surfaces, pole density peaks of $\{21\bar{3}0\}$ were observed.

As mentioned earlier, there is still debate concerning the shape of mineral particles in bone; some experimental results suggest mineral particles are rod-like in shape [5–7] whereas other studies indicate a plate-like shape [8–10] or an elongated platelet shape [25]. In order for a plane such as $\{21\bar{3}0\}$ to have a preferred orientation, the cross-sectional shape of the mineral particle perpendicular to the bone axis would be anisotropic. The mineral particle would not be a rod-like shape but rather a prism shape. Traub et al. [10] and Weiner and Price [9] presented models for the shape of mineral particles in mineralized turkey leg tendon and in bone, respectively, and reported that in both systems, mineral particles were tabular in shape and the table plane had a particular orientation against the collagen fibril. The crystallographic axes relating to such a table plane are expected to also have a particular orientation against the collagen fibril. This expectation relates the morphological model to the biaxial nature of bone mineral particles revealed by the XPFA in this work.

References

1. Katz JL (1981) Composite material models for cortical bone. In: Cowin SC (ed) Mechanical properties of bone. Am Soc Mechanical Eng New York
2. Currey JD (1984) The mechanical adaptations of bones. Princeton University Press, Princeton, NJ
3. Gilmore RS, Katz JL (1982) Elastic properties of apatites. J Mater Sci 17:1131–1141
4. Tanioka A, Tazawa T, Miyasaka K, Ishikawa K (1974) Effects of water on the mechanical properties of gelatin films. Biopolymers 13:735–746
5. Johansen E, Parkes HF (1960) Electron microscope observations on the three-dimensional morphology of apatite crystallites of human dentine and bone. J Biophys Biochem Cytol 7:743–746
6. Bocciarelli DS (1970) Morphology of crystallites in bone. Calcif Tissue Res 5:261–269
7. Fratzl P, Paris O, Klaushofer K, Landis WJ (1996) Bone mineralization in an osteogenesis imperfecta mouse model studied by small-angle X-ray scattering. J Clin Invest 97:396–402
8. Robinson RA (1952) An electron microscope study of the crystalline inorganic component of bone and its relationship to the organic matrix. J Bone Joint Surg 34:389–434
9. Weiner S, Price PA (1986) Disaggregation of bone into crystals. Calcif Tissue Int 39:365–375
10. Traub W, Arad T, Weiner S (1989) Three-dimensional ordered distribution of crystals in turkey tendon collagen fibers. Proc Natl Acad Sci USA 86:9822–9826
11. Glimcher MJ (1984) Recent studies of the mineral phase in bone and its possible linkage to the organic matrix by protein-bound phosphate bounds. Phil Trans R Soc Lond B304:479–508
12. Sasaki N, Matsushima N, Ikawa T, Yamamura H, Fukuda A (1989) Orientation of bone mineral and its role in the anisotropic mechanical properties of bone. Tarnsverse anisotropy. J Biomchanics 22:157–164
13. Wagner HD, Weiner S (1992) On the relationship between the microstructure of bone and its mechanical stiffness. J Biomechanics 25:1311–1320
14. Landis WJ (1995) The strength of a calcified tissue depends in part on the molecular structure and organization of its constituent mineral crystals in their organic matrix. Bone 16:533–544
15. Matsushima N, Akiyama M, Terayama Y (1982) Quantitative analysis of orientation of mineral in bone from small angle X-ray scattering patterns. Jpn J Appl Physiol 21:186–189
16. Lees S (1979) A model for the distribution of hap crystallites in bone. An hypothesis. Calcif Tissue Int 27:53–56
17. Glimcher MJ (1981) On the form and function of bone: from molecules to organs. In: Veis A (ed) The chemistry and biology of mineralized connective tissues. Elsevier North Holland, New York
18. Katz EP, Li S (1973) Structure and function of bone collagen fibrils. J Mol Biol 80:1–5
19. Bonar LC, Glimcher MJ (1981) Supramolecular structure and packing differences between tendon and bone collagens. In: Veis A (ed) The chemistry and biology of mineralized connective tissues. Elsevier North Holland, New York
20. Cowan PM, North ACT, Randall JT (1955) X-ray diffraction studies of collagen fibers. Symp Soc Exp Biol 135:39–51
21. Schultz LG (1949) A direct method of determining preferred orientation of a flat reflection sample using a geiger counter X-ray spectrometer. J Appl Physiol 20:1030–1033
22. Matsushima N, Tokita M, Hikichi K (1986) X-ray determination of the crystallinity in bone mineral. Biochim Biophys Acta 883:574–579
23. Glimcher MJ (1976) Composition, structure and organization of bone and other mineralized tissues and the mechanism of calcification. In: Greep RO, Astwood EB (eds) Handbook of physiology 7—endocrinology VII. American Physiology Society, Washington, DC, pp 15–116
24. Kakudo M, Kasai A (1972) X-ray diffraction by polymers. Kodansha Ltd, Tokyo
25. Lee DD, Glimcher MJ (1991) Three-dimensional spacial relationship between the collagen fibrils and inorganic calcium phosphate crystals of pickerel and herring bone. J Mol Biol 217:487–501